

ENGINEERING STUDIES ON JOINT BAR INTEGRITY, PART II: FINITE ELEMENT ANALYSES

Michael E. Carolan

David Y. Jeong

A. Benjamin Perlman

Volpe National Transportation Systems Center
US Department of Transportation
Cambridge, MA, USA

ABSTRACT

This paper is the second in a two-part series describing research sponsored by the Federal Railroad Administration (FRA) to study the structural integrity of joint bars. In Part I, observations from field surveys of joint bar inspections conducted on revenue service track were presented [1]. In this paper, finite element analyses are described to examine the structural performance of rail joints under various loading and tie-ballast support conditions. The primary purpose of these analyses is to help interpret and understand the observations from the field surveys.

Moreover, the finite element analyses described in this paper are applied to conduct comparative studies and to assess the relative effect of various factors on the structural response of jointed rail to applied loads. Such factors include: discrete tie support (i.e. supported joint versus suspended joint with varying spans between effective ties), bolt pattern (four versus six bolts), initial bolt tension, and easement. In addition, results are shown for 90 lb rail joined with long-toe angle bars compared to 136 lb rail joined with standard short-toe joint bars.

INTRODUCTION

Rail integrity is a topic within the FRA's Track Safety Research Program which deals with the prevention and control of rail failures. Rail failures, or broken rails, usually originate from defects that form and grow as result of metal fatigue. Past rail integrity research focused on defects that occur internally in the rail head of continuous welded rail (CWR) [2, 3]. Previous research on the structural integrity of bolted rail joints has been limited to investigations of bolt-hole cracking [4, 5], and has not been studied as extensively as that in CWR.

Referring to Figure 1, rail joints may be classified as either insulated or bolted joints [6]. Insulated joints may be bonded (in which the joint bars are epoxied to the rail) or non-bonded (which are basically bolted joints with electrical insulating properties). Bolted joints consist of either compromise or standard joints. Compromise bars are used to join two rails of unequal size (e.g. joining 115 lb rail and 140 lb rail). Standard joints may be either temporary or permanent.

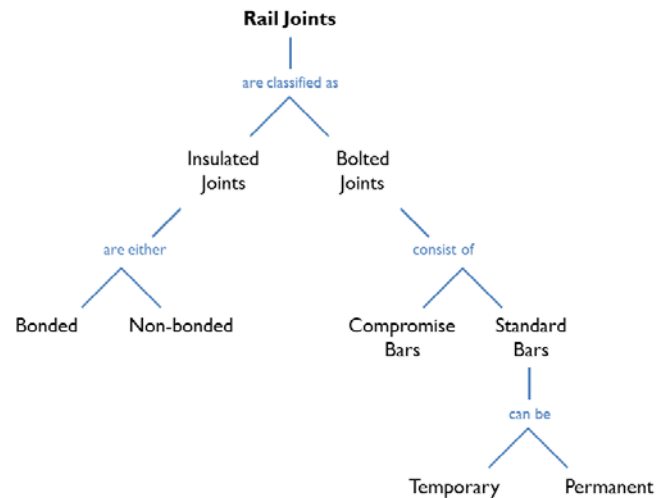


Figure 1: Classification of Rail Joints

Data from the FRA Rail Accident/Incident Reporting System (RAIRS) were presented in Part I [1], exhibiting that the incidents involving joint failures are very rare events. However, several accidents have resulted in severe consequences

involving the release of hazardous materials in some cases and fatalities and injuries to passengers in others. In 2012, the FRA Office of Research and Development initiated a research project to study the structural performance of rail joints and the associated track and operational factors leading to joint bar failures. Field evaluation surveys were conducted to gather measurements on various joints in CWR and jointed rail (JR) territory. Observations and results from statistical analysis of the collected data were summarized in Part I. This paper describes the development of finite element analyses to examine the structural performance of bolted joint rail under applied loading.

Previous finite element analysis (FEA) of rail joints was conducted to calculate live (i.e. bending) stresses in joint bars, which in turn were used to estimate fatigue initiation life of joint bars subjected to vertical loading only [7]. In addition, stresses in rail joints were studied by Applied Rail Research Technologies, which included finite element analysis with the objective to tease out what can be done to reduce and manage the stresses [8, 9, and 10]. However, the previous FEA methods in [7] have since been refined for the purpose of helping to interpret and understand the observations of field surveys of joint bar inspections on revenue service track described in Part I of this two-part series. Testing and analysis of insulated rail joints are being conducted by Virginia Tech and the Transportation Technology Center, Inc. under the sponsorship of the Association of American Railroads [11]. This paper focuses on FEA of bolted rail joints.

MECHANICS OF A RAIL JOINT

In theory, the forces acting on a bolted rail joint depend on several factors such as: joint bar type (e.g. long-toe angle bar or short-toe joint bar), length of the joint bar, rail size, tie-ballast support conditions, bolt tension, number of bolts, and joint anomalies (such as rail end gap, rail height mismatch, tread mismatch, and end batter). The mechanics of a bolted joint must also account for dynamic impact loads.

In terms of structural performance, rail joints are considered as a weak link because the section properties (i.e. cross-sectional area and area moments of inertia) of the bars are typically less than those of the rail itself. For example, Table 1 lists section properties for 90 ARA-A rail and its corresponding long-toe angle bars. Table 2 lists section properties for 136 RE rail and for short-toe joint bars associated with 132 RE rail. These joint bars were originally dedicated to join 132 RE but are often used to join 136 RE and 140 RE rail sections as well.

A consequence of reduced section properties is relatively larger deflection at the joint as wheels pass over it. Further, these large deflections can lead to and accelerate track degradation, which in turn can affect the structural performance of the joint assembly. When a single wheel passes over the joint, the rail ends deflect downward one at a time, creating a small step and mismatch in rail heights. The size of the step varies depending on the original gap distance between rail ends.

The step causes wear from repeated wheel passes, which is referred to as end batter. The rail joint also degrades as the bolts and the supporting ballast loosen. Eventually, increased deflections and joint anomalies (e.g. excessive gap between rail ends, end batter, loose bolts, etc.) induce dynamic amplification of wheel loads at the joint, which accelerates the degradation process. This continuous cycle of deteriorating track and joint conditions leading to and caused by high dynamic wheel impact loads is illustrated schematically in Figure 2.

Table 1: Summary of Section Properties for 90-ARA Rail and Angle Bars

	A_R (in ²)	I_{yy} (in ⁴)	I_{zz} (in ⁴)
Rail 	8.82 ^(a)	38.7 ^(a)	7.41 ^(b)
Long-toe Angle Bars* 	9.68 ^(b)	14.7 ^(b)	6.2 ^(b)

NOTES:

* Properties for two bars

(a) From Foster Rail Catalogue

(b) Estimated

Table 2: Summary of Section Properties for 136 RE Rail and 132 RE Joint Bars

	A_R (in ²)	I_{yy} (in ⁴)	I_{zz} (in ⁴)
Rail 	13.32 ^(a)	94.2 ^(a)	14.5 ^(b)
Short-toe Joint Bars* 	11.78 ^(c)	32.28 ^(c)	3.1 ^(b)

NOTES:

* Properties for two bars

(a) From Foster Rail Catalogue

(b) Estimated

(c) From 1999 AREMA Manual

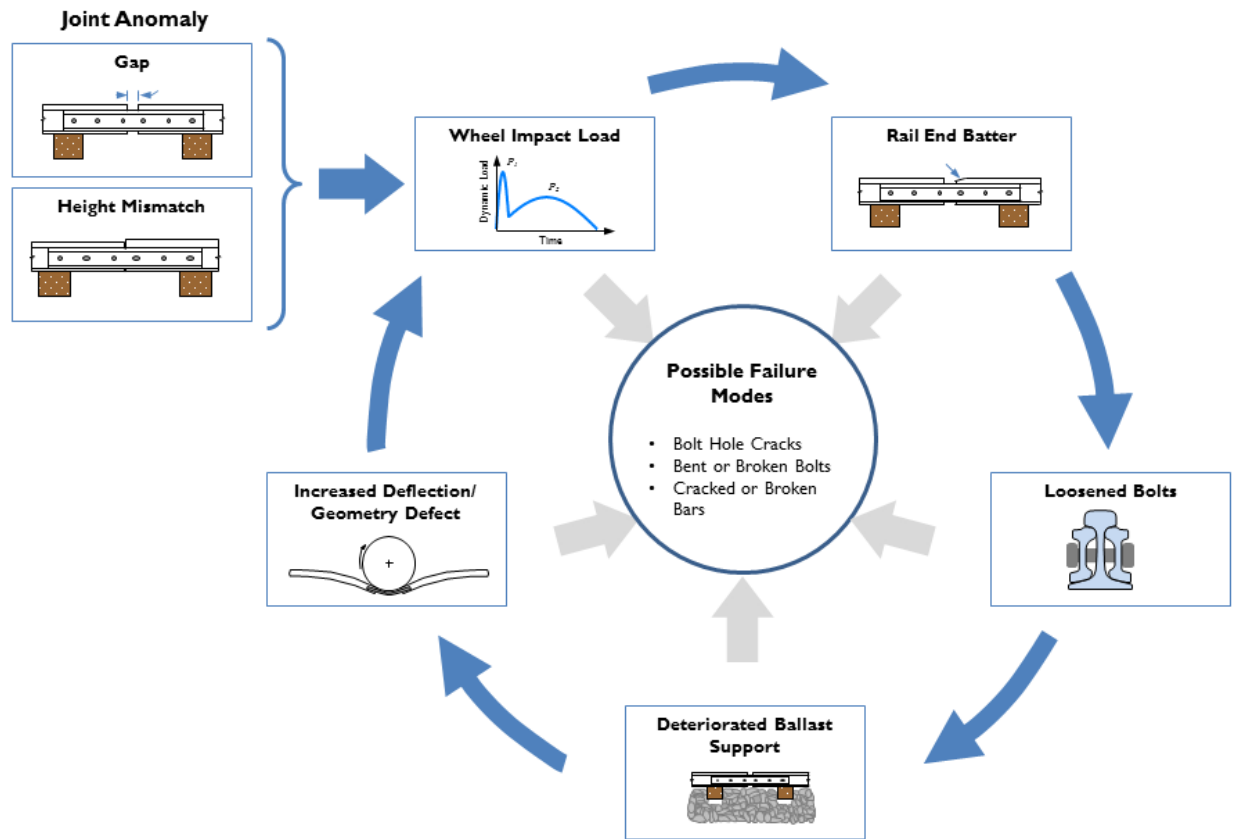


Figure 2: Cycle of Joint and Track Degradation Interacting with Wheel Impact Loads

The schematic in Figure 2 includes wheel/rail impact loads at the joint. Vertical dynamic wheel loads are assumed to consist of a short-time peak (called the P_1 load) and a delayed peak (referred to as the P_2 load) [12]. The short-time peak is associated with battering of the rail end by the unsprung mass of the wheel set. The delayed peak is associated with rail bending, which is a more resilient deformation mode than corner batter. Consequently, P_1 is larger than P_2 , and the difference between them increases as the train speed increases. In addition, the duration of the delayed peak is about four to ten times that of the short-time peak. Moreover, P_1 is related to the inertia of the rail and ties, while P_2 is transmitted to the ballast, which produces track deflections. The results presented in this paper are based on static finite element analysis. Preliminary developmental work is being conducted to examine dynamic effects, which will be a topic for future communications.

COMPARATIVE STUDIES

Finite element analysis (FEA) is an appropriate tool to examine the structural response of bolted rail joints to mechanical loading under varying anomalies and support conditions. Moreover, the objectives of the modeling effort are: to identify potential conditions for failure, to interpret the data

collected during field evaluation surveys which are described in Part I of this two-part series [1], to evaluate “what-if” scenarios, and to provide guidance for future research.

The commercial code ABAQUS is used to carry out the present analyses [13]. Joint components (i.e. bars and bolts) are modeled using three-dimensional solid elements. Rails are also modeled with 3-D solid elements in the vicinity of the joint and with beam elements away from the joint. In addition to bolted rail joints, FEA modeling is carried out for continuous rail. Calculations based on the classical theory of beams on elastic foundation [14] are compared to the FEA results for continuous rail to provide confidence and to verify the modeling approach. Structural performance of rail joints can be examined through joint deflections and stresses in the bars. The total stress in joint bars comprises effects from bending, thermal shrinkage, and residual stresses. Another contributor is bolt tension. When joint bars are applied to rail, they are held in place by a set of nuts and bolts. Torque is applied to each nut to tighten the hardware and keep it in place. The torque also puts the bolt shank into tension. The shank tension is reacted by pressures between the bolt head and the inside face of the nut against the outside faces of the joint bars. The bolts in the joint assembly are assigned initial tensioning.

Table 3 lists the nominal assumptions in the FEA models for bolted rail joints. The static wheel load is based on the maximum gross rail load for freight cars used in the modern-day, heavy-axle load environment (i.e. 286,000 lb divided by eight wheels), or 35.75 kips. Tie spacing and tie spring stiffness are related through an equivalent continuous foundation modulus of 3,000 psi which is a value representative of well-maintained track in revenue service.

Table 3: Nominal Assumptions in FEA Models

Static Wheel Load	35.75 kips
Tie-center Spacing*	20 inches
Tie Spring Stiffness*	60 kips per inch per tie
Rail End Gap	0.125 inch
Initial Bolt Tension	6 kips per bolt

* The combination of tie stiffness and tie-center spacing are based on an equivalent continuous foundation modulus of 3,000 psi.

Figure 3 shows an elevation view of the 4-hole long-toe angle bar (24 inches in length) used for 90 lb rail and of the 6-hole standard joint bar (36 inches in length) used for 136 lb rail. FEA models include all four bolts for the long-toe angle bar. Different bolt patterns are considered for cases involving standard joint bars (e.g. four bolts versus six bolts).

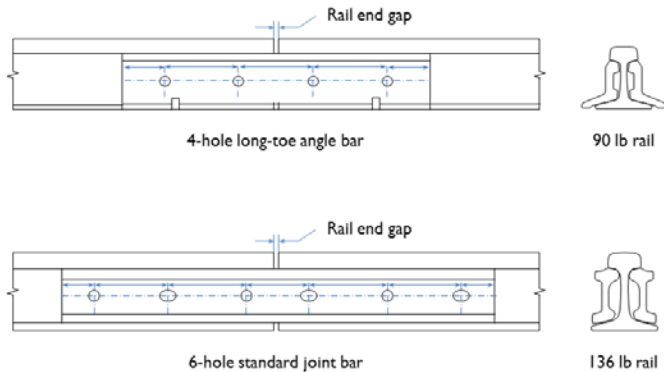


Figure 3: Elevation and Cross Section of Long-toe Angle Bar and Standard Joint Bar

In addition, the finite element modeling is used to examine the effect of an easement at the top of the joint bar.

Discrete Support

Finite element analysis is appropriate and amenable to account for the effect of discretely-spaced crossies. Two aspects of discrete support are considered: (1) supported joint versus suspended joint, and (2) varying the span or distance between effective ties for suspended joints (d in Figure 4). As

shown in the figure, a crossie is located at the center of a supported joint. Varying the span for the suspended joint is intended to approximate the conditions for degraded tie-ballast support.

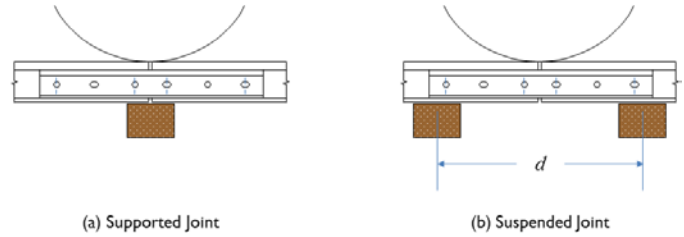


Figure 4: Crosstie Support Conditions at a Rail Joint

Supported joints are expected to have smaller vertical deflections and bending moments than suspended joints because of increased stiffness offered by the tie at the center of the joint. However, one disadvantage of the supported joint is that increased stiffness may result in larger wheel impact forces and therefore increased batter. Conversely, suspended joints will deflect and bend more under load than supported joints.

Table 4 shows FEA results for vertical deflections assuming different track conditions. Nominal assumptions in these results are 136 RE rail supported by a foundation modulus of 3,000 psi, and those listed in Table 3. The vertical deflection of 0.135 inch for continuous rail under load is in perfect agreement with the deflection calculated based on the theory of beams on elastic foundation. The table also shows results for jointed rail, which confirm that deflections are greater for suspended joints than supported joints. The results further show that the number of bolts used to assemble the joint has a negligible effect on the vertical deflection under the assumed conditions.

Table 4: FEA-calculated Joint Deflections for 136 RE rail

Continuous Rail		0.135"
Supported Joint	4 bolts	0.147"
	6 bolts	0.146"
Suspended Joint	4 bolts	0.169"
	6 bolts	0.169"

Profiles of the vertical deflections calculated by FEA are shown in Figure 5 for supported joints and in Figure 6 for suspended joints. Both figures exhibit a discontinuous slope at the center of supported and suspended joints. Previous research conducted by British Rail [9] determined that the dip angle at the joint is directly related to the dynamic impact forces, P_1 and P_2 . These results indicate that dynamic impact forces, in addition to vertical deflections, are greater at suspended joints than supported joints.

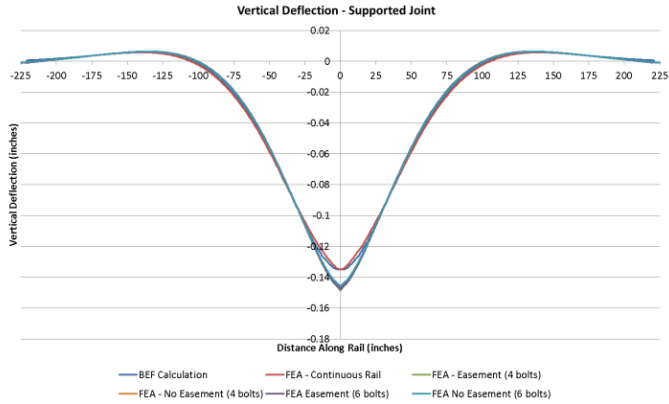


Figure 5: Vertical Deflections along Length of Rail, Supported Joint

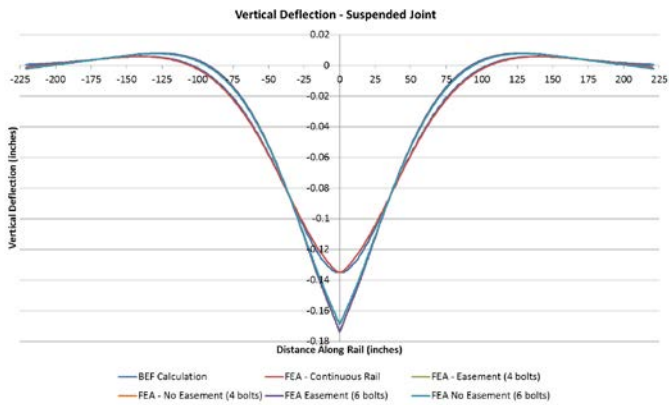


Figure 6: Vertical Deflections along Length of Rail, Suspended Joint

Significant vertical movements (on the order of 2 inches) were observed during the field evaluation surveys conducted in jointed rail territory [1]. Referring back to Figure 2, large vertical deflections might also be indicative of deteriorating or degraded ballast support. Figure 7 shows two schematic diagrams of tie support modeled by linear springs. Degraded support is modeled by assuming a value of 1 kip per inch for tie spring stiffness, K_R , compared to the nominal value, K_T of 60 kips per inch (recall Table 3). In case (a), two ties have reduced stiffness, which translates into a span of 60 inches between effective ties. Case (b) has four ties with reduced stiffness, equal to a distance of 100 inches between effective ties.

Figure 8 shows results from FEA calculations for the vertical deflection profiles under five different track conditions. These results assume 90 lb rail and long-toe angle bars for conditions involving jointed rail. In this plot, distance along the rail is normalized by the tie-center spacing (20 inches), and vertical deflection is normalized by the maximum vertical deflection for the continuous rail. Thus the first track condition,

continuous rail with uniformly spaced ties and all ties with the same stiffness, is the normalizing case. Jointed rail under the same support conditions shows slightly greater vertical deflection. As the support conditions become more degraded, both the continuous rail and the jointed rail experience greater deflections. Under the worst support condition assumed in the analysis (i.e. four ineffective ties), the joint deflection is more than four times the deflection of the continuous rail with nominal support.

Photographs taken during the field surveys show the physical presence of a crosstie near failed or defective joints. The results from the FEA suggest that although the tie may be physically present, it may be incapable of supporting load.

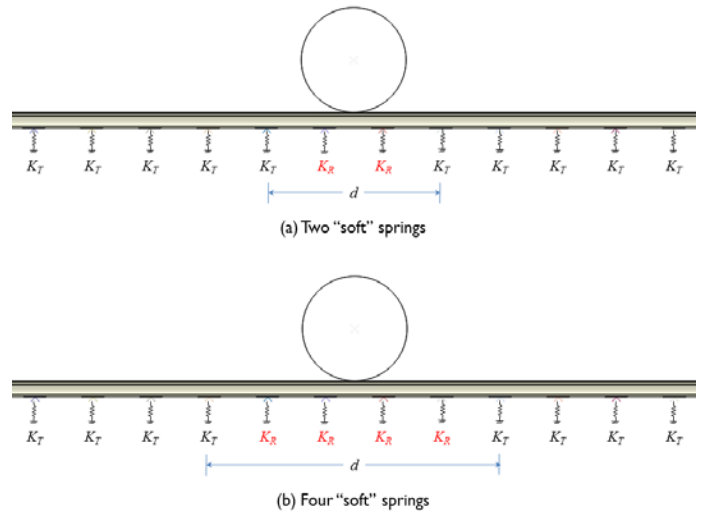


Figure 7: Degraded Support at Joint

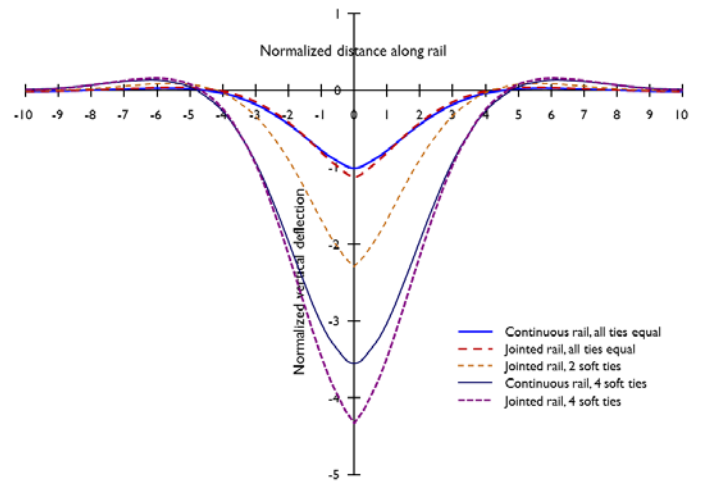


Figure 8: Normalized Vertical Deflection Profiles for Different Track Conditions

Effect of Easement

Observations from the field evaluation surveys reveal that the most common defect found in standard joint bars is cracking at the top center of the bar. Failure of joint bars is presumed to be related to metal fatigue. However, fatigue initiation at the top of the joint bar is counterintuitive. Figure 9 shows a schematic of a joint bar in bending as a wheel passes over it. When the wheel is directly over the center of the joint, the maximum tension in the bar occurs at the bottom while the top of the bar is in compression. The magnitude of the maximum compressive stress for standard joint bar is roughly 90% of the magnitude of the maximum tensile stress due to the centroid location. After the wheel has traveled some distance away from the joint, the nature (i.e. tensile versus compressive) of the bending stress reverses; the top of the bar is in tension while the bottom of the bar is in compression. The schematic in Figure 9 shows the bending stress cycles for the top and the bottom of the bar assuming a reverse bending factor of 20 percent. This value is based on the maximum reverse bending calculated from the theory of beams on elastic foundation, which may be an overestimate. Moreover, comparison of the stress cycles at the top and the bottom of the bar indicate that cracking should initiate at the bottom of the bar because tensile stresses, in theory, are more damaging than compressive stresses. In other words, metal fatigue alone cannot explain why crack initiation occurs at the top of the bar. Two factors come to mind that affect crack initiation at the top of the bar: lack of easement and residual stress.

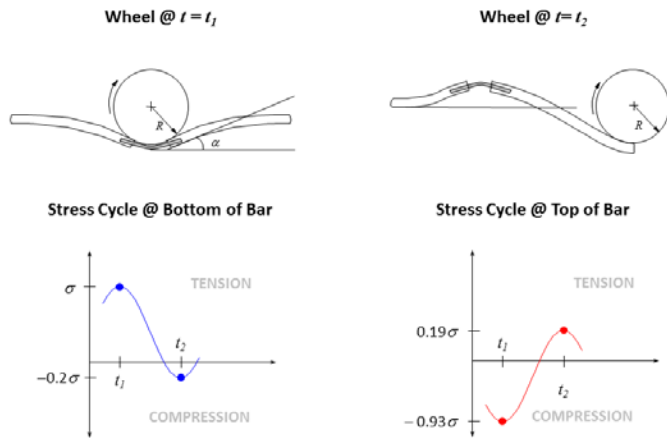


Figure 9: Schematic of Joint Bar in Bending

In the context of joint bars, an easement is a recessed portion or depression in the bar, presumably intended to reduce the possibility of rail end contact with the top of the joint bar. Figure 10 shows the AREMA recommendation for easement in head-free joint bars [15]. If the joint bar does not have an easement, or if the easement is not properly aligned, knife-edge

contact between the rail ends and the top of the bar could create an area of local stress concentration to initiate failure.

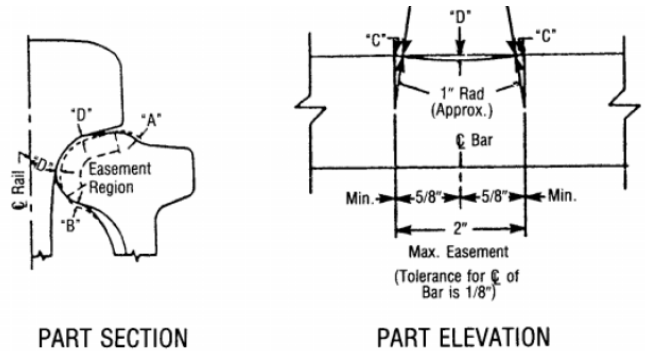


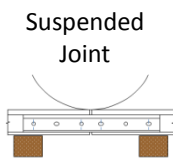
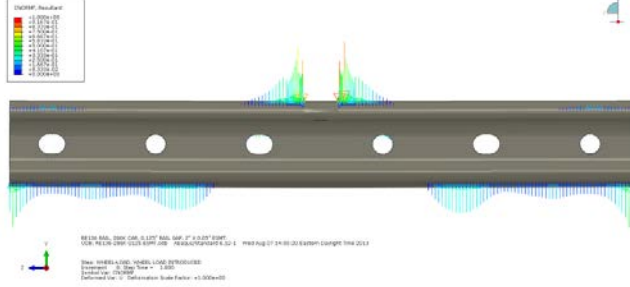
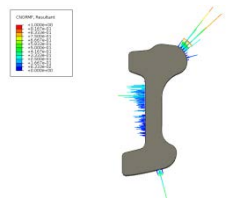
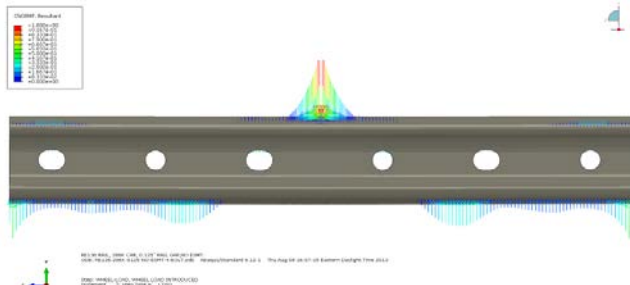
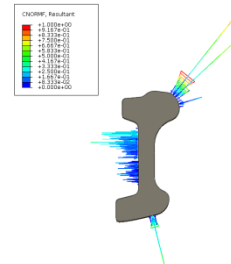
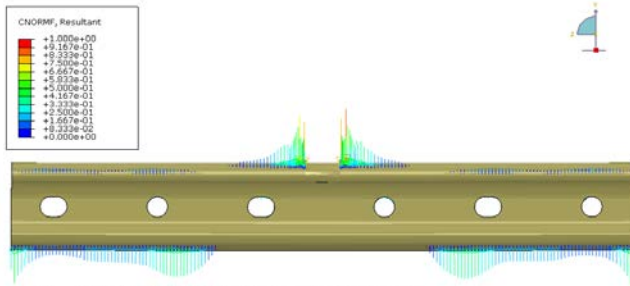
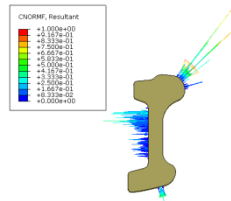
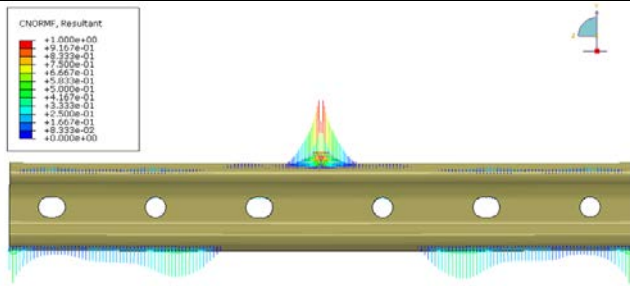
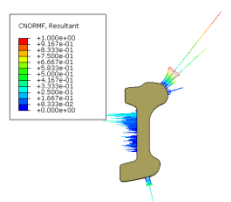
Figure 10: Recommended Head Easement for Head-Free Joint Bars [12]

The effect of the head easement is examined by using FEA to calculate contact forces and pressures between the bar and the rail. Although FEA was conducted for both supported and suspended joints, only results for suspended joints are presented in this paper. In the results that follow, the number of bolts is varied (4 versus 6 bolts) with and without the easement in 6-hole standard joint bars connecting 136 lb rail. Table 5 shows elevation views for contact forces acting on standard joint bars. The contact forces acting on the top of the bar have a triangular shape with a sharp peak or maximum value. The maximum contact forces are higher in bars without the easement than in bars with the easement. Contours of contact pressures greater than 1 psi acting on the joint bar and 136 lb rail are presented in Table 6. Contact pressures are shown to be greatest adjacent to the easement. Furthermore, contact pressure on the bottom of the joint bar is lower than on the top for either case. High contact stresses are likely to cause plastic flow, which may ultimately lead to initiation of cracking.

Bolt tension was also calculated using FEA. A nominal value of initial tension was assigned to each bolt in the assembly, prior to any externally applied loads. Tension in the bolts was then calculated when the wheel is located directly over the center of the joint. Table 7 shows bar graphs for bolt tension before and after the wheel load is applied. In all suspended joint cases, bolt load increases in every bolt when the wheel load is introduced. Independent of whether 4 or 6 bolts are used in the assembly, the two inner-most bolts are shown to have the greatest increase in tension. In all supported joint cases, bolt load decreases in every bolt when the wheel load is introduced.

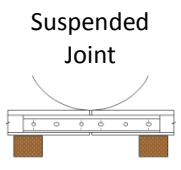
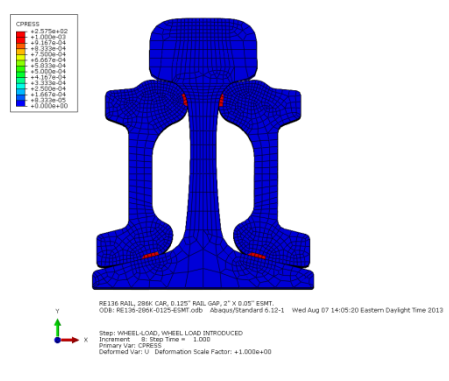
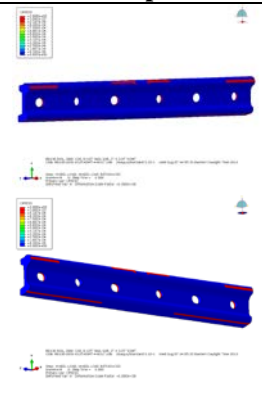
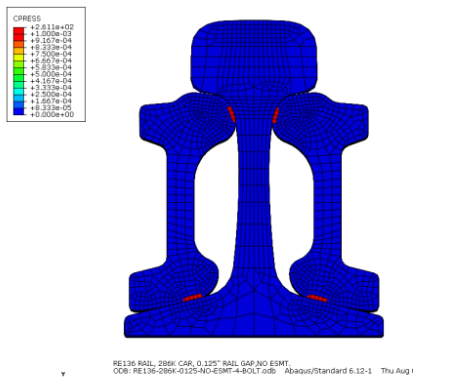
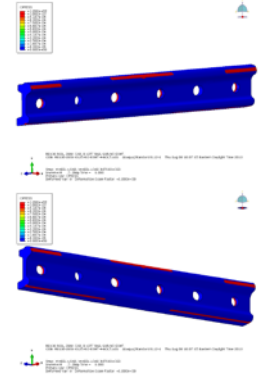
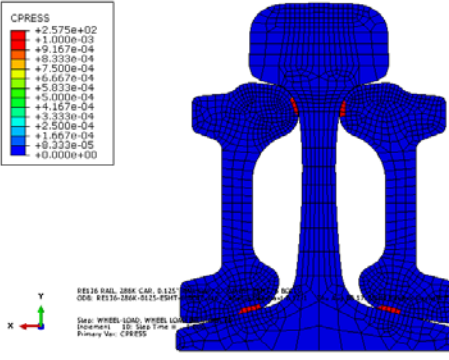
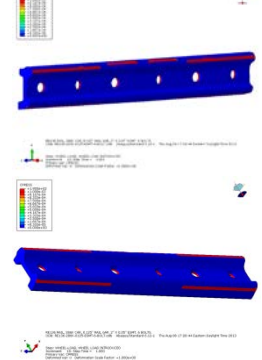
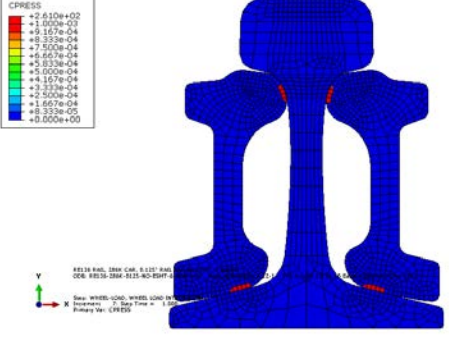
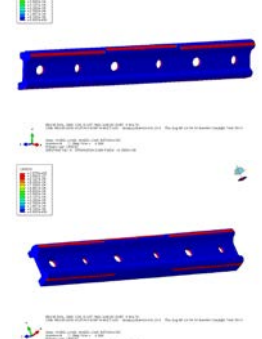
Measurements of residual stresses in joint bars were conducted by the Transportation Technology Center, Inc. [16]. Residual stresses are generally compressive at the top of the rail. However, the effect of residual stresses was not examined in the present FEA study.

Table 5. Contact Force Normal to Element Faces on Joint Bar (Suspended Joint)

 <p>Suspended Joint</p>	4 bolts Easement		
	4 bolts No Easement		
	6 bolts Easement		
	6 bolts No Easement		

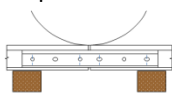
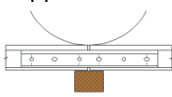
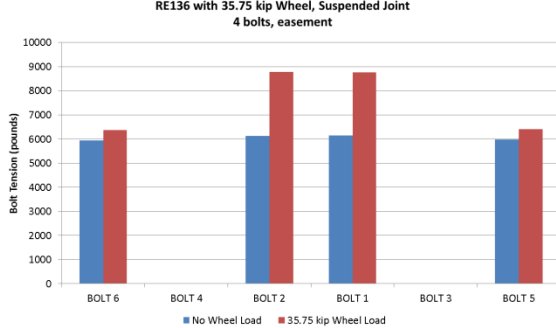
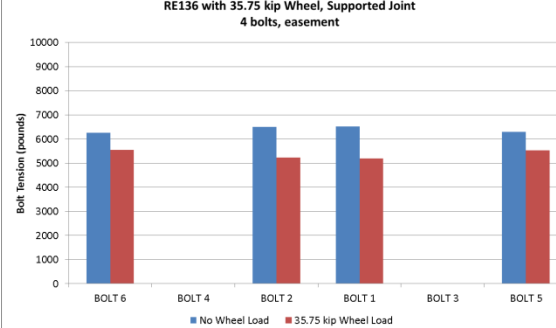
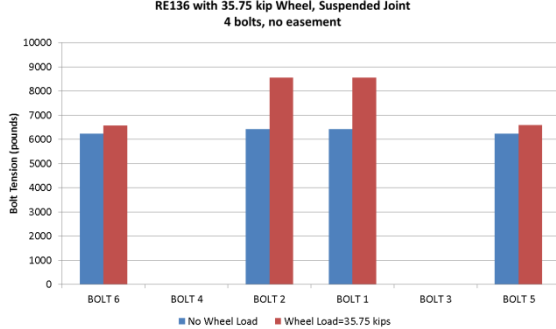
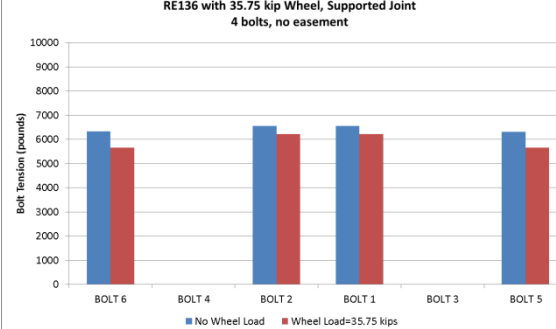
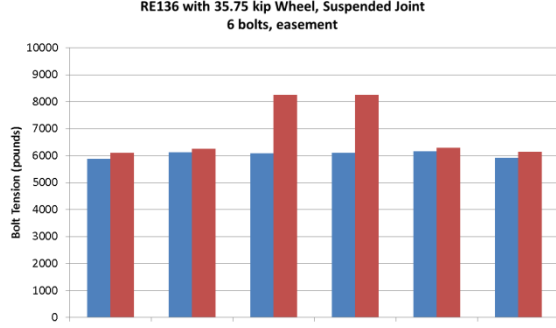
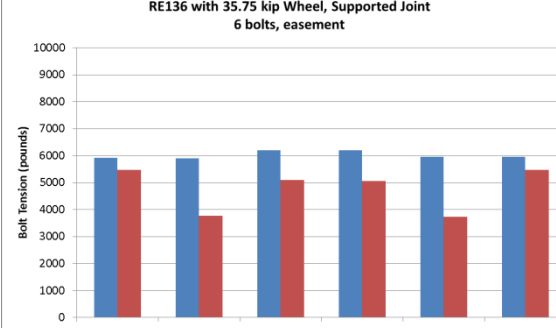
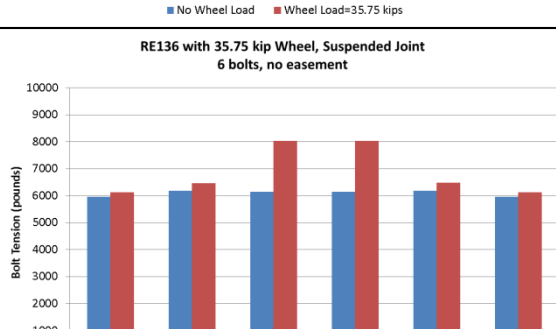
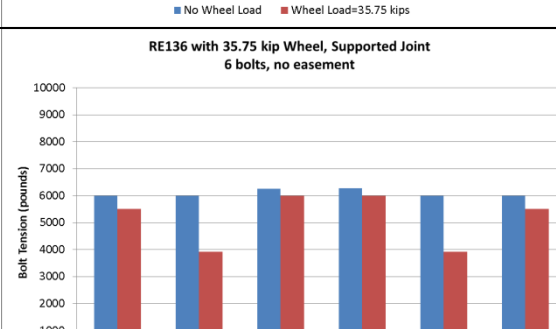
Note: Maximum contour for all cases set at 1,000 lbs.

Table 6. Contours of Contact Pressure Greater than 1 psi (Suspended Joint under 35.75-kip Wheel Load)

 <p>Suspended Joint</p>	<p>4 bolts Easement</p>	 <p>FEA mesh of rail joint with 4 bolts and easement. Legend: CRESS values from +2.611e+02 to +0.000e+00.</p>	 <p>Two views of rail joint with 4 bolts and easement showing contact pressure contours.</p>
	<p>4 bolts No Easement</p>	 <p>FEA mesh of rail joint with 4 bolts and no easement. Legend: CRESS values from +2.611e+02 to +0.000e+00.</p>	 <p>Two views of rail joint with 4 bolts and no easement showing contact pressure contours.</p>
	<p>6 bolts Easement</p>	 <p>FEA mesh of rail joint with 6 bolts and easement. Legend: CRESS values from +2.575e+02 to +0.000e+00.</p>	 <p>Two views of rail joint with 6 bolts and easement showing contact pressure contours.</p>
	<p>6 bolts No Easement</p>	 <p>FEA mesh of rail joint with 6 bolts and no easement. Legend: CRESS values from +2.610e+02 to +0.000e+00.</p>	 <p>Two views of rail joint with 6 bolts and no easement showing contact pressure contours.</p>

Note: Contours set to indicate pressure greater than 1 psi.

Table 7. Bolt Tension in Each Joint Before and After 35.75-kip Wheel Load

	Suspended Joint 	Supported Joint 
4 bolts Easement	RE136 with 35.75 kip Wheel, Suspended Joint 4 bolts, easement 	RE136 with 35.75 kip Wheel, Supported Joint 4 bolts, easement 
4 bolts No Easement	RE136 with 35.75 kip Wheel, Suspended Joint 4 bolts, no easement 	RE136 with 35.75 kip Wheel, Supported Joint 4 bolts, no easement 
6 bolts Easement	RE136 with 35.75 kip Wheel, Suspended Joint 6 bolts, easement 	RE136 with 35.75 kip Wheel, Supported Joint 6 bolts, easement 
6 bolts No Easement	RE136 with 35.75 kip Wheel, Suspended Joint 6 bolts, no easement 	RE136 with 35.75 kip Wheel, Supported Joint 6 bolts, no easement 

CONCLUDING REMARKS

This paper described results from finite element analyses of bolted rail joints under varying scenarios. Finite element analysis (FEA) of continuous rail (i.e. without a bolted joint) were also conducted, and were found to be in excellent agreement with classical analysis based on the theory of beams on elastic foundation.

Moreover, FEA was applied to examine: the differences between supported and suspended joints, the effect of degraded support conditions in the vicinity of the joint on vertical deflection, bolt tension when the joint is under load, and contact forces acting on a bar with and without an easement.

Future work will consider: (1) development of models for compromise bars, (2) the effect of lateral load, and (3) dynamic (i.e. moving) wheel load.

NOMENCLATURE

A_R	Cross-sectional area for entire rail
d	Distance between effective ties in suspended joint
I_{yy}	Area moment of inertia for vertical bending
I_{zz}	Area moment of inertia for lateral bending
K_T	Tie stiffness
K_R	Reduced tie stiffness
k_V	Vertical foundation modulus
P_1	Short-time peak impact force
P_2	Delayed peak impact force

ACKNOWLEDGMENTS

The work described in this paper was sponsored by the Office of Research and Development, Federal Railroad Administration (FRA), U.S. Department of Transportation, under the direction of Mr. Gary Carr, Chief of the Track Research Division.

REFERENCES

1. Jeong, D.Y., Bruzek, R., Akhtar, M., Tajaddini, A., "Engineering Studies of Joint Bar Integrity, Part I: Field Surveys and Observed Failure Modes," *Proceedings of the 2014 Joint Rail Conference*, Colorado Springs, CO, JRC2014-3706, April 2014.
2. Orringer, O., et al., "Crack Propagation Life of Detail Fractures in Rails," Volpe Center Final Report to Federal Railroad Administration, DOT/FRA/ORD-88-13, October 1988.
3. Jeong, D.Y., Tang, Y.H., Orringer, O., "Damage tolerance analysis of detail fractures in rail," *Theoretical and Applied Fracture Mechanics* 28, 109-115 (1997).
4. Mayville, R.A., Hilton, P.D., "Fracture mechanics analysis of a rail-end bolt hole crack," *Theoretical and Applied Fracture Mechanics* 1, 51-60 (1984).
5. Mayville, R.A., Stringfellow, R.G., "Numerical analysis of a railroad bolt hole fracture problem," *Theoretical and Applied Fracture Mechanics* 24, 1-12 (1995).
6. Akhtar, M., Davis, D.D., "Load Environment of Rail Joints – Phase I: Effects of Track Parameters on Rail Joint Stresses and Crack Growth," Transportation Technology Center, Inc. Final Report to Federal Railroad Administration, DOT/FRA/ORD-13-24 (2013). <http://www.fra.dot.gov/eLib/details/L04515>
7. Talamini, B., Jeong, D.Y., Gordon, J.E., "Estimation of the Fatigue Life of Railroad Joint Bars," *Proceedings of the 2007 ASME/IEEE Joint Rail Conference & Internal Combustion Engine Spring Technical Conference*, Pueblo, CO, JRCICE2007-40065, March 2007. <http://ntl.bts.gov/lib/35000/35200/35229/jrcice2007-40065.pdf>
8. Igwemezie, J., Nguyen, A.T., "Anatomy of joint bar failures I," *Railway Track and Structures*, 31-37, July 2009.
9. Igwemezie, J., Nguyen, A.T., "Anatomy of joint bar failures II," *Railway Track and Structures*, 43-48, October 2009.
10. Igwemezie, J., Nguyen, A.T., "Anatomy of joint bar failures III," *Railway Track and Structures*, 31-36, February 2010.
11. Iranmanesh, A.H., West, R.L., Ahmadian, M., "Insulated Railroad Joint Design Evaluation by Coordinated Test and Finite Element Analysis," *Proceedings of the ASME 2013 Rail Transportation Division Fall Technical Conference*, Altoona, PA, RTDF2013-4715, October 2013.
12. Jenkins, H.H., et al., "The effect of track and vehicle parameters on wheel/rail vertical dynamics forces," *Railway Engineering Journal* 3, 2-26 (1974).
13. ABAQUS/Standard 6.12, Dassault Systèmes Simulia Corp., Providence, RI, 2012.
14. Hetényi, M., *Beams on Elastic Foundation*, University of Michigan Press, Ann Arbor, MI, 1974.
15. AREMA Manual for Railway Engineering, Vol. 1, Track, American Railway Engineering and Maintenance-of-Way Association (1999).
16. Akhtar, M., et al., "Load Environment of Rail Joints – Phase II: Joint Bar Service Failure Prevention," Transportation Technology Center, Inc. Draft Report to Federal Railroad Administration (2013).